

A Novel Cell Ablation Strategy Blocks Tobacco Anther Dehiscence

Thomas P. Beals and Robert B. Goldberg¹

Department of Molecular, Cell, and Developmental Biology, University of California, Los Angeles, California 90095-1606

We utilized a new cell ablation strategy to ablate specific anther cell types involved in the dehiscence process. The tobacco *TA56* gene promoter is active within the circular cell cluster, stomium, and connective regions of the anther at different developmental stages. We introduced a cytotoxic *TA56/barnase* gene into tobacco plants together with three different anticytotoxic *barstar* genes. The anticytotoxic *barstar* genes were used to protect subsets of anther cell types from the cytotoxic effects of the *TA56/barnase* gene. The chimeric *barstar* genes were fused with (1) the tobacco *TP12* gene promoter that is active at high levels in most anther cell types; (2) the soybean *lectin* gene promoter that is active earlier in the connective, and at lower levels in the circular cell cluster and stomium, than is the *TA56* promoter; and (3) the tobacco *TA20* gene promoter that is active at high levels in most anther cell types but has a different developmental profile than does the *TP12* promoter. Normal anther development and dehiscence occurred in plants containing the *TA56/barnase* and *TP12/barstar* genes, indicating that *barstar* protects diverse anther cell types from the cytotoxic effects of *barnase*. Anthers containing the *TA56/barnase* and *lectin/barstar* genes also developed normally but failed to dehisce because of extensive ablation of the circular cell cluster, stomium, and contiguous connective regions. Anthers containing the *TA56/barnase* and *TA20/barstar* genes failed to dehisce as well. However, only the stomium region was ablated in these anthers. The connective, circular cell cluster, and adjacent wall regions were protected from ablation by the formation of *barnase/barstar* complexes. We conclude that anther dehiscence at flower opening depends on the presence of a functional stomium region and that chimeric *barnase* and *barstar* genes containing promoters that are active in several overlapping cell types can be used for targeted cell ablation experiments.

INTRODUCTION

Anther development can be divided into two general phases (Koltunow et al., 1990; Goldberg et al., 1993, 1995). During the first phase, the stamen is partitioned into the anther and filament, specialized anther cell types differentiate from three primordial cell layers, the anther acquires its characteristic bilateral shape, four microsporangia and accessory cell types form, and microspore mother cells within each microsporangium undergo meiosis to produce haploid microspores (Goldberg et al., 1993, 1995). The second phase is characterized by enlargement of the anther, elongation of the filament, pollen grain differentiation, and a cell degeneration and dehiscence program that terminates with the release of mature pollen grains at flower opening (Keijzer, 1987a, 1987b; Bonner and Dickinson, 1989, 1990; Goldberg et al., 1993, 1995). Although much progress has been made in dissecting the genetic events that control stamen specification (Weigel and Meyerowitz, 1994; Yanofsky, 1995), little information exists regarding the mechanisms that control the differentiation of diverse anther cell types, the switch from a histodifferentiation/morphogenesis program (phase one) to a cell death and

dehiscence program (phase two), and the processes responsible for ensuring that anther development is complete and pollen release occurs at the time of flower opening.

Pollen grains are released after breakage of a specific anther region, the stomium, at dehiscence (Keijzer, 1987a, 1987b; Bonner and Dickinson, 1989, 1990). The stomium is a specialized cell layer that runs along the lateral side of each anther half, or theca, as shown schematically in Figure 1. In tobacco, stomium initials differentiate from specific epidermal founder cells that reside between the two locules of each theca (P.M. Sanders, T.P. Beals, and R.B. Goldberg, unpublished results). Figure 1 (stage 1) shows that these stomium initials are in a shallow notch, or indentation, in the anther wall between the two locules. These initial cells divide periclinally during phase two of anther development, giving rise to a three-tiered stomium that is flanked on each side by larger epidermal cells (Figure 1, stages 4 and 6). Bright-field photographs of transverse tobacco anther sections showing the notched stomium region at different stages of anther development are presented in Figure 2A.

A unique set of cells, designated as the circular cell cluster (Koltunow et al., 1990; Goldberg et al., 1993, 1995), the intersporangial septum (Bonner and Dickinson, 1989), or the

¹To whom correspondence should be addressed. E-mail bobg@ucla.edu; fax 310-825-8201.

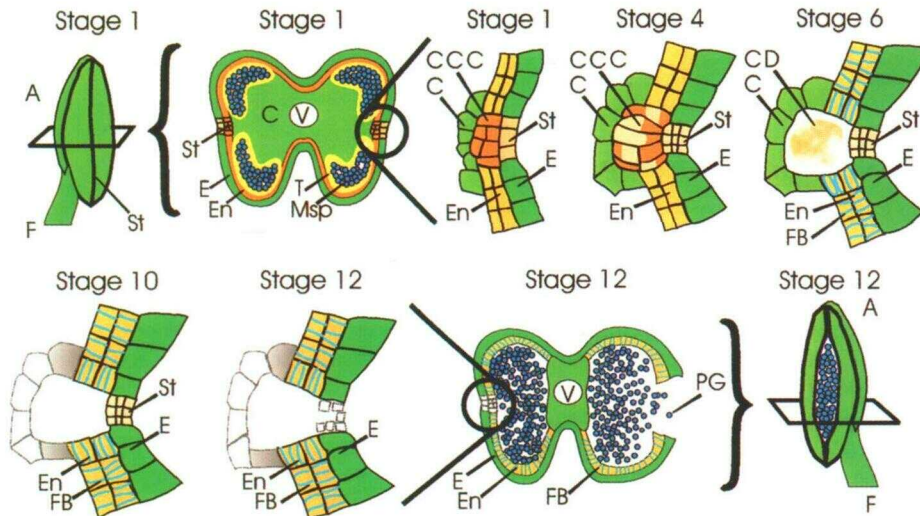


Figure 1. An Overview of Stomium and Circular Cell Cluster Development in the Tobacco Anther.

Schematic representations of stomium and circular cell cluster differentiation are based on histological studies at the light and electron microscopy levels (Koltunow et al., 1990; P.M. Sanders, S.H. Tu, and R.B. Goldberg, unpublished results). The major events that occur at different stages of tobacco anther development have been described previously (Koltunow et al., 1990). Colors depict different cell types and cell layers within the anther. The circles highlight cells in the stomium region between each pollen chamber. Brackets represent the transverse cross-section of the anther depicted in stages 1 and 12. The rectangles drawn around the stage 1 and stage 12 anther cartoons represent the cross-section plane for the anther regions drawn for stages 1, 4, 6, 10, and 12. A, anther; C, connective; CCC, circular cell cluster; CD, cell debris; E, epidermis; En, endothecium; F, filament; FB, fibrous bands; Msp, microspores; PG, pollen grains; St, stomium; T, tapetum; V, vascular bundle.

hypodermal stomium (Horner and Wagner, 1992), is associated with the stomium in tobacco and other solanaceous plants (Figures 1 and 2A). The circular cell cluster is composed of specialized idioblast cells that accumulate calcium oxalate crystals (Bonner and Dickinson, 1989; Horner and Wagner, 1992). The precise role, if any, that these calcium crystal-containing idioblasts play in anther development is not known. As shown conceptually in Figure 1 (stage 1), the circular cell cluster develops from founder cells immediately below the epidermal initials that give rise to the stomium (P.M. Sanders, T.P. Beals, and R.B. Goldberg, unpublished results). The circular cell cluster initials divide and elongate during phase two (stages 1 to 4), generate large calcium oxalate-containing vacuoles, and undergo a cell death program between stages 4 and 6 before anther dehiscence (Figures 1 and 2A). Cell debris, including calcium crystals, persists after the circular cell cluster has degenerated at stage 6 (Figures 1 and 2A). Differentiation of both the circular cell cluster and the stomium is marked by new gene expression programs (Koltunow et al., 1990). The developmental period in which the circular cell cluster degenerates is also characterized by the appearance of fibrous bands, or cell wall thickenings, in the endothecium and adjacent wall layers (Figures 1 and 2A). Degeneration of the circular cell cluster and connective permits the two locules of each theca to become confluent and form a large unified chamber so that

pollen grains can be released from the single stomium region (Figures 1 and 2A).

It is not known what genes and processes control the specification of stomium and circular cell cluster initials from contiguous founder cells within the anther primordium (Goldberg et al., 1993, 1995). Neither is it known what mechanisms restrict stomium and circular cell cluster differentiation to the intersporangial regions of the anther and what mechanisms and genes are responsible for stomium breakage and release of pollen grains at flower opening. We hypothesized previously that stomium and circular cell cluster initials interact with each other and/or adjacent cell types and that these interactions are responsible in part for directing these initials to follow stomium and circular cell cluster differentiation pathways within the interlocular region (Goldberg et al., 1993, 1995).

As a first step in investigating the differentiation of the circular cell cluster and stomium and the roles that these regions play in the anther dehiscence process, we initiated a set of experiments designed to ablate these cell types during anther development. Targeted cell ablation experiments with either a microbeam laser (Sulston et al., 1983) or chimeric cytotoxic genes (Palmiter et al., 1987) can be used to determine the function of a given cell type as well as to determine whether cell-cell interactions play a role in the cell differentiation process (Day and Irish, 1997). One of the difficulties

in using chimeric cytotoxic genes for cell ablation studies is the requirement for cell-specific promoters, that is, promoters that are active only in the target cell type. In many cases, promoters that are active in the target cell type are also active in other cell types, either preventing the generation of transgenic individuals or complicating the interpretation of the ablation experiments (Goldberg et al., 1995; Day and Irish, 1997). Previously, we used the *Bacillus amyloliquefaciens barnase* and *barstar* genes (Hartley, 1988, 1989) to genetically engineer a new system of male fertility control in higher plants (Mariani et al., 1990, 1992). *Barstar* binds specifically with barnase, forming highly stable barnase/*barstar* complexes that inhibit barnase ribonuclease activity (Hartley, 1989; Schreiber and Fersht, 1995). We showed that a chi-

meric *barstar* gene containing the tobacco tapetal-specific *TA29* promoter (Koltunow et al., 1990) could inhibit the cytotoxic effects of a *TA29/barnase* gene within anther tapetal cells and restore fertility to male-sterile plants (Mariani et al., 1992).

In this study, we show how a novel cell ablation strategy can be used to ablate specific anther cell types (Goldberg et al., 1995). We show that the *barnase* and *barstar* genes can be fused to promoters with different but overlapping cell specificities to ablate either the stomium and the circular cell cluster or the stomium region alone, leading to anthers that fail to dehisce. Our results demonstrate that a set of functional stomium cells is required for anther dehiscence and pollen release at flower opening.

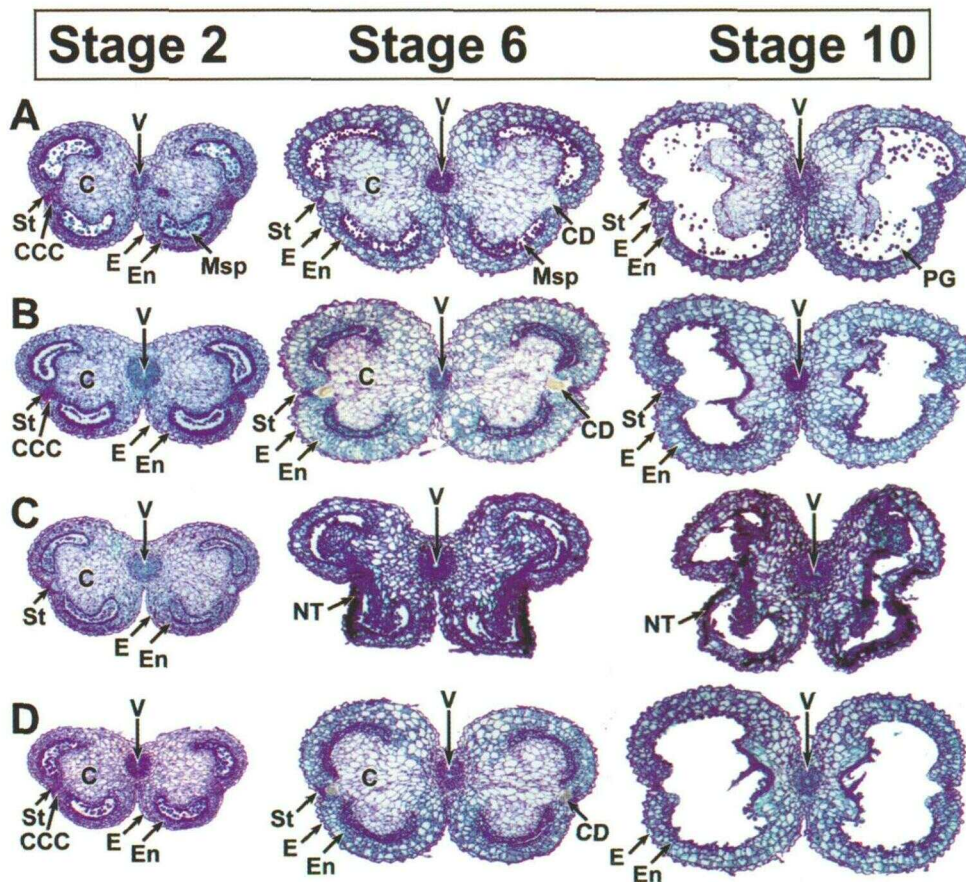


Figure 2. Development of Wild-Type Anthers and Transgenic Anthers Containing Chimeric *Barnase* and *Barstar* Genes.

(A) Anther sections from wild-type plants.

(B) Anther sections from plants containing the *TA56/barnase* and *TP12/barstar* genes.

(C) Anther sections from plants containing the *TA56/barnase* and *lectin/barstar* genes.

(D) Anther sections from plants containing the *TA56/barnase* and *TA20/barstar* genes.

C, connective; CCC, circular cell cluster; CD, cell debris; E, epidermis; En, endothecium; Msp, microspores; NT, necrotic tissue; PG, pollen grains; St, stomium; V, vascular bundle.

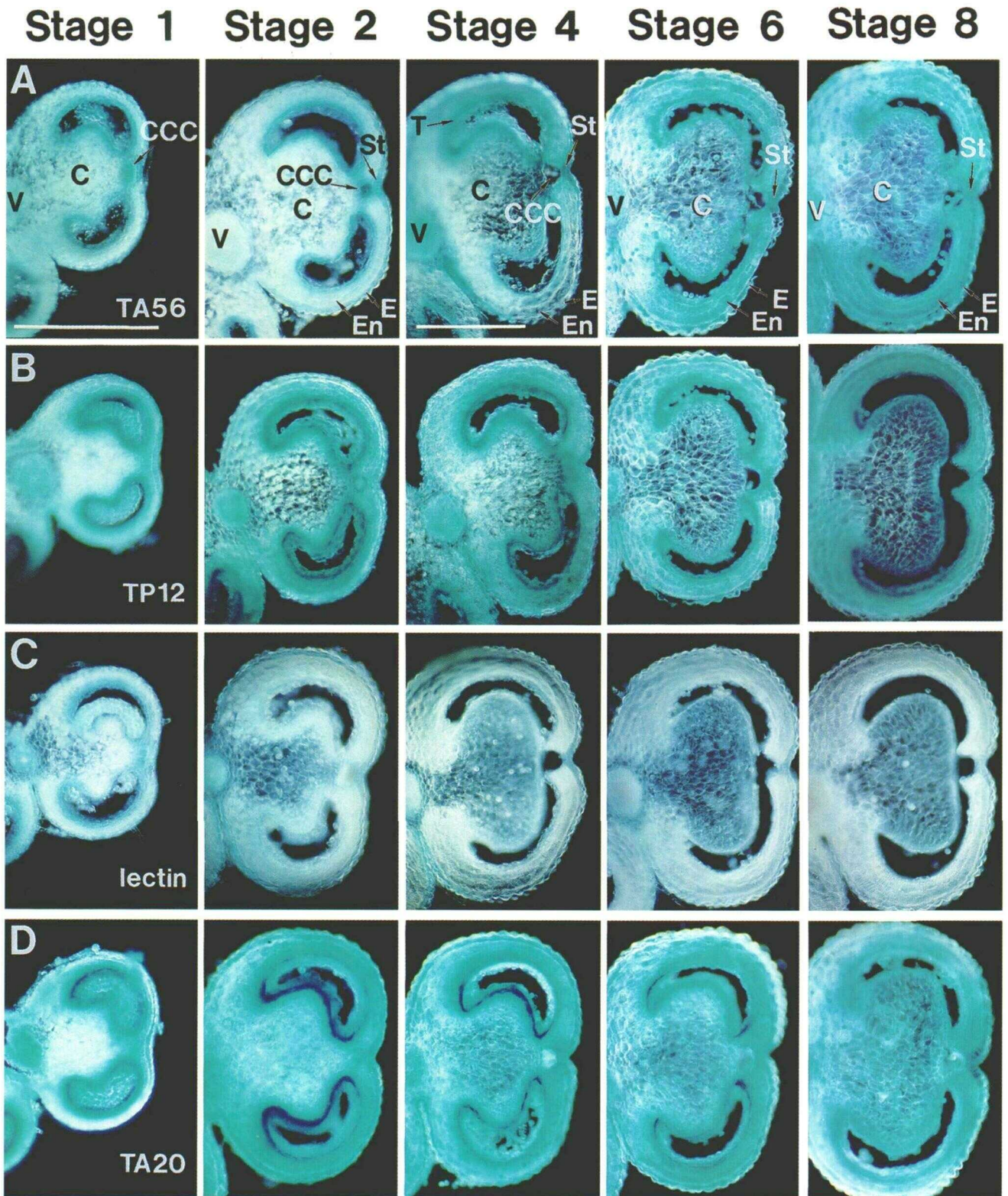


Figure 3. Localization of GUS Enzyme Activity in Transgenic Anthers Containing Different Chimeric *GUS* Genes.

RESULTS

The Tobacco *TA56* Gene Promoter Is a Transcriptional Marker for the Stomium and Circular Cell Cluster

We previously identified a thiol endopeptidase gene, designated *TA56*, that is active during phase two of tobacco anther development and is a marker for the stomium and circular cell cluster (Koltunow et al., 1990). *TA56* mRNA accumulates first in the circular cell cluster, then in the stomium, and finally within the connective before anther dehiscence and pollen release (Koltunow et al., 1990). We fused an 830-bp *TA56* gene promoter region (see Methods) with the *Escherichia coli* β -glucuronidase (*GUS*) reporter gene (Jefferson et al., 1987) and then transferred the *TA56/GUS* gene to tobacco plants to determine whether the cell-specific *TA56* mRNA accumulation pattern was controlled at the transcriptional level (see Methods).

Figure 3A shows that at stage 1 of anther development, blue color resulting from *GUS* enzyme activity was visualized in the circular cell cluster as well as in the tapetum, cells surrounding the locules, and the vascular bundle. At stage 2, the blue color was very intense within the circular cell cluster relative to other cell types. At stage 6, a dark blue color was observed in the stomium and connective, whereas a lower level of *GUS* activity was visualized in the anther wall and vascular tissue. No blue staining was observed within the circular cell cluster because this region of the anther degenerated by stage 6 (Figures 1 and 2A). A similar pattern of *TA56/GUS* gene transcriptional activity was observed in the anthers of four independent transformants (data not shown). We conclude that the cell-specific *TA56* mRNA accumulation pattern within the anther is controlled primarily by transcriptional events.

A Strategy for Targeted Cell Ablation Studies Using *Barnase* and *Barstar* Genes

We wanted to exploit the transcriptional activity of the *TA56* gene promoter within the stomium and circular cell cluster in

order to use cell ablation experiments to investigate the function of these regions in the dehiscence process as well as the potential interactions between these regions during their differentiation. We could not use a chimeric *TA56* cytotoxic gene alone to ablate the circular cell cluster and/or stomium because the *TA56* promoter was active in other anther cell types (Figure 3A). In fact, transferring a *TA56/barnase* gene containing the 830-bp *TA56* promoter to tobacco leaf disks failed to yield transgenic plants (data not shown). Callus derived from *TA56/GUS* plants containing the same 830-bp promoter (see Methods) produced an intense blue color resulting from *GUS* enzyme activity, indicating that the *TA56* promoter was active in the callus and that the failure to obtain *TA56/barnase* plants was probably due to the cytotoxic effects of barnase at the callus stage (data not shown).

Figure 4 illustrates conceptually the cell ablation strategy that we used to overcome the problems associated with using the *TA56* gene promoter and other promoters that are active in multiple cell types (Goldberg et al., 1995). This strategy uses the two-component *barnase/barstar* gene system driven by promoters with overlapping but different cell specificities to suppress the cytotoxic effects of barnase in non-target cell types (Mariani et al., 1990, 1992; Goldberg et al., 1993, 1995). One promoter is fused to the *barstar* gene (Figure 4A), whereas the second promoter is fused to the *barnase* gene (Figure 4B). Both promoters are active in a common, non-target cell type (Figure 4, square cells in upper right quadrant). The promoter driving the *barnase* gene, however, is active in an additional cell type, the target cell (Figures 4A to 4C, round cells in lower right quadrant). Introducing the chimeric *barnase* and *barstar* genes simultaneously into these cells results in (1) the production of barnase/barstar complexes in the common, or shared, cell type and (2) the production of barnase alone in the target cell type (Figure 4C). The non-target cell type is protected from the cytotoxic effects of barnase by the production of barnase/barstar complexes (Figure 4D). By contrast, the target cell type is ablated by barnase cytotoxic activity because barstar is absent from these cells (Figure 4D). In principle, this strategy should permit us to use the *TA56/barnase* gene to ablate the stomium and/or circular cell cluster in combination with additional

Figure 3. (continued).

DNA fragments containing the *TA56* promoter (A), the *TP12* promoter (B), the *lectin* promoter (C), or the *TA20* promoter (D) were fused with the *GUS* coding region and transferred to tobacco plants, as outlined in Methods. Anthers from different developmental stages were harvested from each transformant, sliced freehand into 100- μ m sections, and assayed for *GUS* activity, as described in Methods. Anthers were assayed from at least four independent transgenic lines per chimeric *GUS* gene. The degenerated circular cell cluster region within the freehand-cut anther sections at stages 4 to 8 appears either as a hole or as a plug of cell debris.

(A) Localization of *GUS* enzyme activity in anthers containing the *TA56/GUS* gene.

(B) Localization of *GUS* enzyme activity in anthers containing the *TP12/GUS* gene.

(C) Localization of *GUS* enzyme activity in anthers containing the *lectin/GUS* gene.

(D) Localization of *GUS* enzyme activity in anthers containing the *TA20/GUS* gene.

C, connective; CCC, circular cell cluster; E, epidermis; En, endothecium; St, stomium; T, tapetum; V, vascular bundle. *TA56*, *TP12*, *lectin*, and *TA20* refer to chimeric *GUS* genes, respectively. Bar in (A), stage 1 = 0.5 mm for (A) to (D), stages 1 and 2; bar in (A), stage 4 = 0.5 mm for (A) to (D), stages 4, 6, and 8.

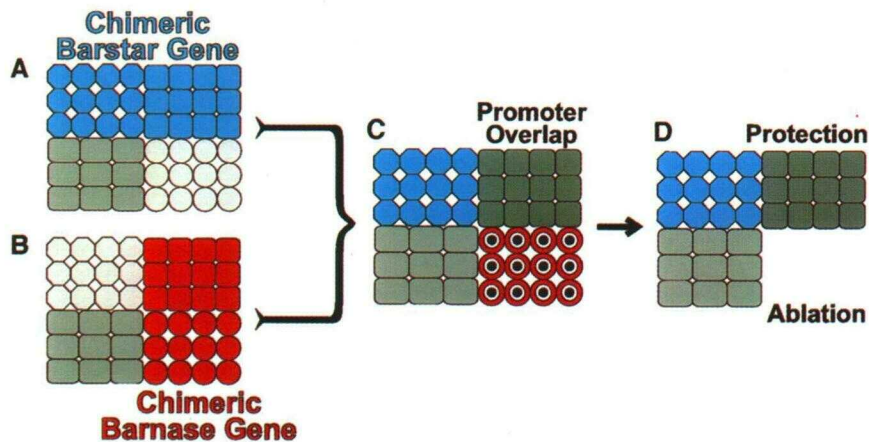


Figure 4. A Cell Ablation Strategy Using Chimeric *Barnase* and *Barstar* Genes with Overlapping Cell Specificities.

Blocks represent cross-sections through a hypothetical organ system that has four different cell types. The circular cells in the lower right quadrants are the targets of the ablation experiment.

(A) Blue represents transcriptional activity of the promoter fused with the anti-cytotoxic *barstar* gene.

(B) Red represents transcriptional activity of the promoter fused with the cytotoxic *barnase* gene.

(C) Combined transcriptional activities of the chimeric *barnase* and *barstar* genes. Both chimeric genes are active within the dark gray cells in the upper right quadrant. Only the chimeric *barnase* gene is active in the target cells present in the lower right quadrant.

(D) Selective ablation of the target cells. *Barnase/barstar* complexes are formed within the dark gray cells in the upper right quadrant protecting them from the cytotoxic effects of *barnase*. The target cells in the lower right quadrant have been ablated selectively due to the cell-specific activity of *barnase*.

promoters that can be fused with the *barstar* gene to suppress the effects of *TA56/barnase* gene activity in other anther regions (e.g., connective). The only requirement for making this strategy work is that the promoter driving the *barstar* gene must have a transcriptional activity equal to or greater than the *TA56* promoter in the non-target cell type; that is, the promoter must be able to generate an excess of *barstar* molecules so that all *barnase* molecules are driven into nontoxic *barnase/barstar* complexes (Hartley, 1989).

Stomium and Circular Cell Cluster Development Occurs Normally in Anthers Containing *TA56/barnase* and *TP12/barstar* Genes

To determine whether the dual-gene ablation strategy presented in Figure 4 could be used to study stomium and circular cell cluster differentiation, it was essential to establish that functional *barnase/barstar* complexes could form in these cell types and other cells of the anther in addition to the tapetum (Mariani et al., 1990, 1992). We identified previously a tobacco mRNA, designated as *TP12*, that accumulates to high levels in the petal and in several anther cell types, including those in the connective and wall layers, depending on the developmental stage (Drews et al., 1992; T.P. Beals and R.B. Goldberg, unpublished results). The *TP12* gene encodes a tobacco homolog of the potato *pata-tin* gene (Drews et al., 1992). Figure 3B shows that a *TP12/*

GUS gene containing a 2-kb *TP12* promoter region (Drews et al., 1992) produced an intense blue color in most anther cell types at different stages of anther development, including the connective, stomium, and circular cell cluster. Similar results were obtained with several independent transgenic lines (data not shown). In addition, callus from plants containing the *TP12/GUS* gene stained dark blue (data not shown). Quantitative measurements of GUS enzyme activity indicated that the *TP12* promoter was at least as strong as the *TA56* promoter when averaged over the entire anther (data not shown). These results suggested that the *TP12* promoter should direct the production of high levels of *barstar* mRNA throughout the anther and in regenerating callus of transgenic plants.

We fused the 2-kb *TP12* promoter with the *barstar* gene, combined the *TP12/barstar* and *TA56/barnase* genes on one plasmid, and introduced the two chimeric genes simultaneously into tobacco cells (see Methods). In contrast with using the *TA56/barnase* gene alone, we obtained many kanamycin-resistant plantlets from leaf discs treated with *Agrobacterium* containing both the *TA56/barnase* and *TP12/barstar* genes (data not shown). We transferred 11 transgenic plants from tissue culture to the greenhouse. Each contained from one to three unrearranged copies of the *TA56/barnase* and *TP12/barstar* genes and was similar to untransformed wild-type plants with respect to growth rate, height, overall morphology, and flowering time (data not shown). The corolla limb region (Drews et al., 1992) of one

transgenic line, however, failed to develop normally (data not shown).

We sectioned anthers at different developmental stages to compare stomium and circular cell cluster differentiation in untransformed wild-type anthers with that in anthers containing the *TA56/barnase* and *TP12/barstar* genes. Figure 2B shows that anthers containing the *TA56/barnase* and *TP12/barstar* genes were indistinguishable from wild-type anthers (Figure 2A) with respect to overall shape, number of diverse cell types (including the stomium and circular cell cluster), and degeneration of the circular cell cluster and connective during phase two of anther development. Figures 5A and 5B show close-ups of the stomium and circular cell cluster regions in wild-type anthers (Figure 5A) and in anthers containing the *TA56/barnase* and *TP12/barstar* genes (Figure 5B) at stages 1, 2, 4, and 10 (Koltunow et al., 1990). No detectable differences from the wild type were observed for stomium and circular cell cluster development in anthers containing the *TA56/barnase* and *TP12/barstar* genes (Figures 5A and 5B). At stage 1, developing circular cell cluster and stomium cells were visualized within the anther intersporangial region. By stage 4, a prominent stomium notch was observed, the circular cell cluster had begun to degenerate, and fibrous bands were present in the endothecium and wall layers. By stage 10, the circular cell cluster had degenerated, a multitiered stomium region was present, and large numbers of fibrous bands were present in cells of the wall layers. Similar results were obtained with sections from several independent transgenic lines (data not shown). Together, these results suggest (1) that the *TP12/barstar* gene can protect regenerating callus from barnase cytotoxic activity during the transformation process and is a dominant suppressor of *TA56/barnase* gene activity and (2) that barnase/barstar complexes can form in most anther regions, including the stomium, circular cell cluster, and connective, that is, regions where both the *TA56* and *TP12* promoters are active.

Anthers Containing the *TA56/barnase* and *TP12/barstar* Genes Dehiscence Normally

We examined the external structure of anthers at different developmental stages and the timing of dehiscence in both wild-type plants and plants containing the *TA56/barnase* and *TP12/barstar* genes. Figure 6A shows the appearance of wild-type anthers at different developmental stages. A prominent stomium notch was visualized along the lateral theca edge by stage 3, and this region split at stage 12, releasing pollen grains from the anther (Figure 6A). As shown in Figure 6B, both the appearance of the stomium notch and the timing of the dehiscence process were similar to that of the wild type (Figure 6A) in anthers containing the *TA56/barnase* and *TP12/barstar* genes. No detectable pollen grains were released from these anthers, however, when the stomium split at stage 12; that is, the plants were male sterile (Figure 6B). Ten of the 11 plants containing the *TA56/bar-*

nase and *TP12/barstar* genes produced no viable pollen. Examination of anther cross-sections from these lines indicated that tetrads formed but that developing pollen grains degenerated after formation of the exine walls (Figure 5B and data not shown).

A small amount of pollen was produced in one transgenic line. This pollen was used to pollinate the pistils of wild-type plants, and viable seeds were produced. Approximately 75% of these seeds produced kanamycin-resistant seedlings, suggesting the presence of two independently segregating kanamycin resistance (T-DNA) loci. Approximately half of the kanamycin-resistant seedlings matured into plants that produced low pollen levels similar to that of the parental transgenic line containing the *TA56/barnase* and *TP12/barstar* genes, whereas the other kanamycin-resistant seedlings produced anthers with wild-type amounts of pollen. When we applied wild-type pollen to the pistils of the same transgenic line, similar kanamycin resistance segregation ratios were obtained, indicating that the male-sterile/low-pollen phenotype was associated with the presence of the *TA56/barnase* and *TP12/barstar* genes. Together, these results indicate (1) that the *TA56/barnase* gene is active in plants containing the *TA56/barnase* and *TP12/barstar* genes, as indicated by their male-sterile phenotype, and (2) that anthers containing the *TA56/barnase* and *TP12/barstar* genes undergo a normal dehiscence process; that is, dehiscence is unaffected by the presence of barnase/barstar complexes in diverse anther cell types.

Barnase and Barstar mRNAs Are Present in Anthers Containing the *TA56/barnase* and *TP12/barstar* Genes

We conducted a series of in situ hybridization experiments to detect barstar and barnase mRNAs in anthers containing the *TA56/barnase* and *TP12/barstar* genes (see Methods). We hybridized adjacent sections of stage 4 anthers from one transgenic line with barnase and barstar anti-mRNA probes and, as a control, with a TP12 anti-mRNA probe. Figure 7A shows the localization pattern for endogenous TP12 mRNA. As predicted by our previous TP12 mRNA localization studies (Drews et al., 1992; T.P. Beals and R.B. Goldberg, unpublished results), a high level of TP12 mRNA was present throughout the anther connective region at this stage of development. As shown in Figure 7B, barstar mRNA was also present within the connective region and to a lesser extent was present within the wall layers. By contrast, Figure 7C shows that no detectable hybridization grains above background were observed within the stage 4 anther sections with the barnase anti-mRNA probe. Nor were we able to detect barnase mRNA in anther sections at other developmental stages in this transgenic line (data not shown).

We utilized the reverse transcriptase-polymerase chain reaction (RT-PCR) with primers specific for the *barnase* gene coding sequence to demonstrate directly that barnase mRNA was present in the anthers of this transgenic line (see

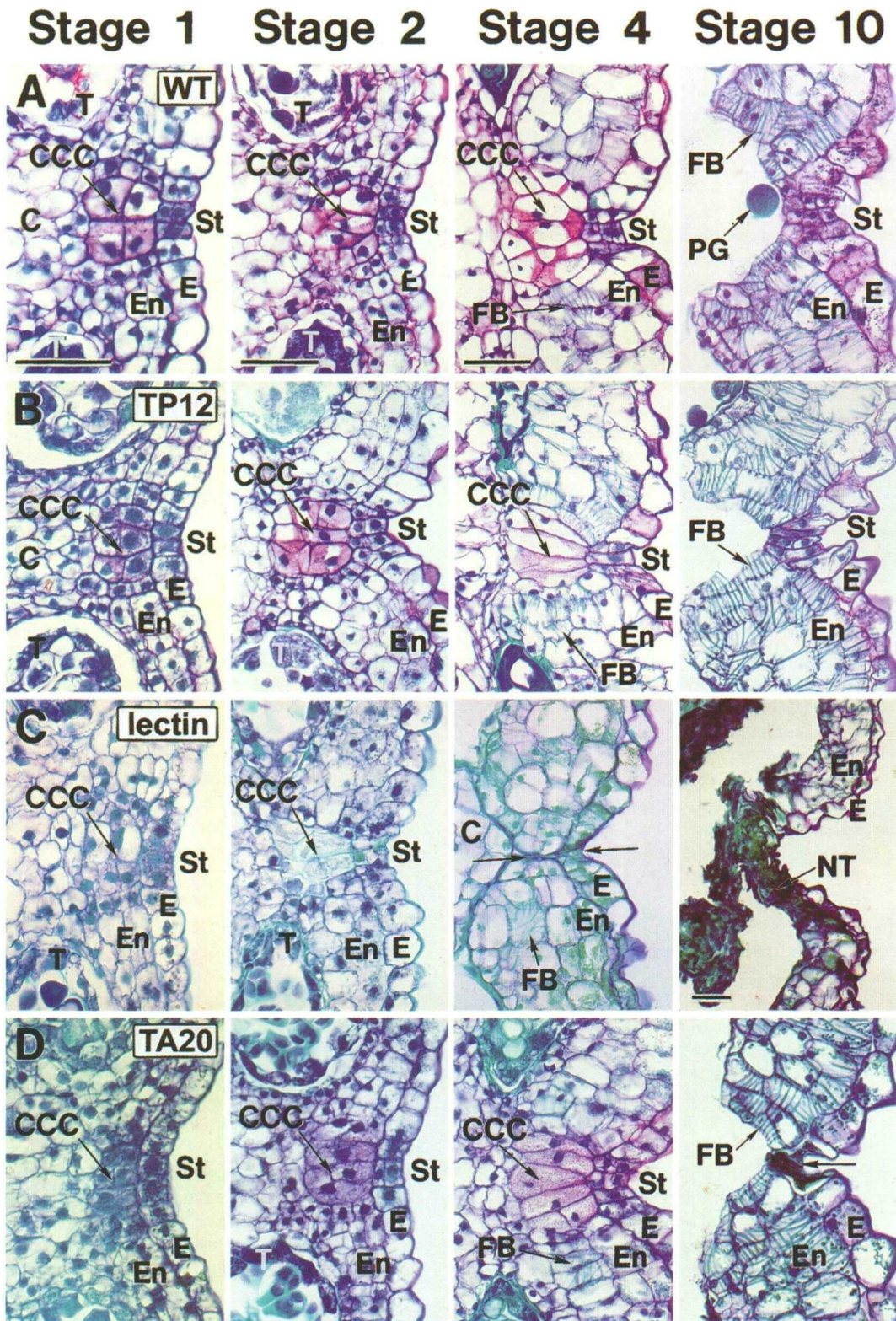


Figure 5. The Stomium and Circular Cell Cluster Regions in Wild-Type Anthers and Transgenic Anthers Containing Chimeric *Barnase* and *Barstar* Genes.

Methods). Figure 8 (lane 19) shows that a 161-bp barnase RT-PCR product was obtained with stage 4 anther RNA. By contrast, the barnase RT-PCR product was not generated with either stage 4 anther RNA in the minus reverse transcriptase control (data not shown) or RNA from stage 4 wild-type anthers (Figure 8, lane 18). As expected from the in situ hybridization experiments (Figure 7), a 398-bp RT-PCR product specific for TP12 mRNA (Figure 8, lanes 2 and 3) was produced with both wild-type anther RNA (Figure 8, lane 2) and RNA from anthers containing the *TA56/barnase* and *TP12/barstar* genes (Figure 8, lane 3). We were able to distinguish the TP12 mRNA RT-PCR product from genomic DNA contaminants by using TP12 primers that flanked an intron in the *TP12* gene (Figure 8, lane 1). In addition, we were able to detect a 394-bp RT-PCR product specific for TA56 mRNA at stage 4 in wild-type anthers (Figure 8, lane 6) and in anthers containing the *TA56/barnase* and *TP12/barstar* genes (Figure 8, lane 7), as predicted by their normal phenotypes (Figures 5A and 5B). Together, these data indicate that (1) both barstar and barnase mRNAs are present within anthers containing the *TA56/barnase* and *TP12/barstar* genes, (2) barstar mRNA is present at a higher level than is barnase mRNA in the transgenic line investigated, and (3) endogenous TP12 and TA56 mRNAs are protected from degradation by the presence of barnase/barstar complexes.

The Stomium and Circular Cell Cluster Are Ablated in Anthers Containing *TA56/barnase* and *lectin/barstar* Genes

We utilized a chimeric *lectin/barstar* gene in combination with the *TA56/barnase* gene to determine whether we could protect regenerating transformants from barnase cytotoxic activity and, in addition, ablate specific anther regions. Previous experiments with the soybean *lectin* gene promoter indicated that it is active at different levels in vegetative and floral organs of transgenic tobacco plants in addition to its strong activity during embryo development (Okamuro et al., 1986; Lindstrom et al., 1990; Yadegari, 1996; R. Yadegari and R.B. Goldberg, unpublished results). Figure 3C shows that a *lectin/GUS* gene containing a 4-kb *lectin* promoter

(Goldberg et al., 1983; Yadegari, 1996; R. Yadegari and R.B. Goldberg, unpublished results) was active at low levels in several anther regions at different developmental stages. For example, the *lectin* promoter was active in the circular cell cluster, in cells on the wall side of the locule, and in the vascular bundle at stage 1 (Figure 3C). *lectin/GUS* gene activity persisted in the vascular bundle at stage 2 but decreased in activity in the other anther cell types (Figure 3C). At later stages of anther development (e.g., stage 6), *lectin/GUS* gene activity was detectable only within the connective (Figure 3C). Similar patterns of GUS enzyme activity were observed within the anthers of four independent *lectin/GUS* transgenic lines (data not shown).

The timing, level, and location of *lectin/GUS* gene activity (Figure 3C) differed with respect to those observed with the *TA56/GUS* gene (Figure 3A) and the *TP12/GUS* gene (Figure 3B). In general, the blue color resulting from GUS enzyme activity was less intense within most cell types of anthers containing the *lectin/GUS* gene (Figure 3C) as compared with anthers containing either the *TA56/GUS* gene (Figure 3A) or the *TP12/GUS* gene (Figure 3B). Quantitative measurements of GUS enzyme activity indicated that when averaged over the anther as a whole, the *lectin* promoter was less active than were both the *TA56* and *TP12* promoters during stages 1 to 10 of anther development (data not shown).

We fused the 4-kb *lectin* gene promoter to the *barstar* gene, combined the *lectin/barstar* and *TA56/barnase* genes on one plasmid, and introduced the two chimeric genes simultaneously into tobacco cells (see Methods). A large number of kanamycin-resistant plantlets were regenerated from leaf discs, indicating that the *lectin/barstar* gene was active and, like the *TP12/barstar* gene, was a dominant suppressor of *TA56/barnase* gene activity during the transformation and plant regeneration process. We transferred 16 independent lines of kanamycin-resistant plantlets to the greenhouse. DNA gel blot studies showed that each transgenic plant contained one or two unrearranged copies of the *TA56/barnase* and *lectin/barstar* genes (data not shown). In general, plants containing the *TA56/barnase* and *lectin/barstar* genes resembled both wild-type plants and plants containing the *TA56/barnase* and *TP12/barstar* genes with respect to height,

Figure 5. (continued).

(A) Anther sections from wild-type plants.

(B) Anther sections from plants containing the *TA56/barnase* and *TP12/barstar* genes.

(C) Anther sections from plants containing the *TA56/barnase* and *lectin/barstar* genes. The arrows at stage 4 point to the ablated circular cell cluster and stomium regions.

(D) Anther sections from plants containing the *TA56/barnase* and *TA20/barstar* genes. The arrow at stage 10 points to the ablated stomium region. C, connective; CCC, circular cell cluster; E, epidermis; En, endothecium; FB, fibrous bands; NT, necrotic tissue; PG, pollen grain; St, stomium; T, tapetum. Magnification in (C), stage 10, shows the extent of ablation in relation to wall structures. WT refers to untransformed anthers. TP12, lectin, and TA20 refer to chimeric *barstar* genes, respectively. Bars in (A), stages 1, 2, and 4 = 50 μ m for the same stages in (B), (C), and (D). Bar in (A), stage 4, also = 50 μ m for (A), (B), and (D), stage 10.

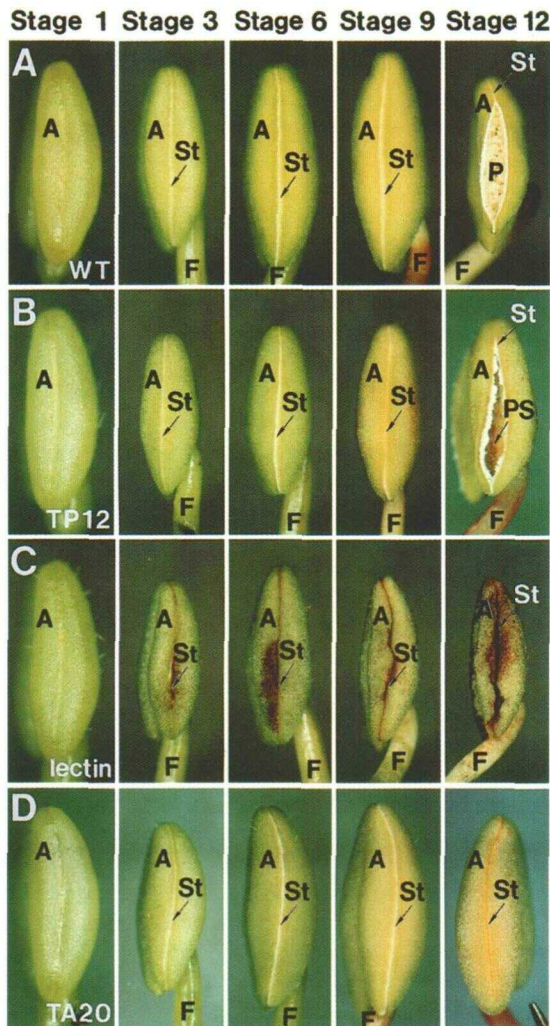


Figure 6. Anther Dehiscence in Wild-Type Anthers and Transgenic Anthers Containing Chimeric *Barnase* and *Barstar* Genes.

Stamens were harvested from flower buds at different developmental stages and then photographed with a dissecting microscope using bright-field illumination. Stamens were photographed at $\times 64$ for stage 1 and $\sim \times 32$ for stages 3, 6, 9, and 12.

(A) Wild-type anthers.

(B) Transgenic anthers containing the *TA56/barnase* and *TP12/barstar* genes.

(C) Transgenic anthers containing the *TA56/barnase* and *lectin/barstar* genes.

(D) Transgenic anthers containing the *TA56/barnase* and *TA20/barstar* genes.

A, anther; F, filament; P, pollen; PS, pollen sac; St, stomium. WT refers to untransformed plants. TP12, lectin, and TA20 refer to chimeric *barstar* genes, respectively.

flowering time, and organ system morphology (data not shown). The lower leaves of plants containing the *TA56/barnase* and *lectin/barstar* genes senesced and abscised prematurely, however, suggesting that *TA56/barnase* cytotoxic activity disrupted the physiological state of older leaves (data not shown). In addition, one transgenic line exhibited extensive floral bud drop at developmental stages 1 to 4 (Koltunow et al., 1990), which resulted in a reduced number of mature flowers per plant (data not shown).

We sectioned anthers containing the *TA56/barnase* and *lectin/barstar* genes to determine whether any anther regions and/or cell types were ablated. Figure 2C shows that stage 2 anthers resembled those of the wild type (Figure 2A) with respect to overall shape, spectrum of diverse anther cell types, and presence of well-differentiated locule regions. By contrast, significant ablation of the cells along the outer edges of the connective and in the wall layers within and adjacent to the stomium region was observed at stages 6 and 10 of anther development (Figure 2C). Higher magnification bright-field photographs of transverse anther sections containing the *TA56/barnase* and *lectin/barstar* genes are shown in Figure 5C. Normal-looking stomium cells were present in stage 1 anthers. By contrast, abnormalities were observed within the circular cell cluster region at this stage in comparison to that of wild-type anthers (Figure 5A) and anthers containing the *TA56/barnase* and *TP12/barstar* genes (Figure 5B). For example, the cell elongation axis was orthogonal to that observed in a wild-type circular cell cluster region (Figures 5A and 5C). At stage 2, both the circular cell cluster and stomium had begun to degenerate prematurely in anthers containing the *TA56/barnase* and *lectin/barstar* genes, and by stage 4, both cell regions were ablated completely (Figure 5C). By contrast, other anther cell types did not differ detectably from those in either wild-type anthers or anthers containing the *TA56/barnase* and *TP12/barstar* genes at similar developmental stages (Figures 2A to 2C and 5A to 5C). At later stages, fibrous bands did not appear within the endothecium (Figures 2C and 5C), and cells of the anther wall and connective within the interlocular regions were ablated, resulting in shrinkage of the anthers (Figures 2C and 5C). Similar phenotypes were observed with the anthers of several independent *TA56/barnase* and *lectin/barstar* transgenic lines (data not shown).

We hybridized anther sections from one transgenic line with a *TA56* anti-mRNA probe to determine whether ablation of the circular cell cluster resulted in a loss of *TA56* mRNA within these cells. As shown in Figure 9, strong *TA56* mRNA signals were observed at stage 2 within the circular cell cluster of wild-type anthers (Figure 9A) and anthers containing the *TA56/barnase* and *TP12/barstar* genes (Figure 9B). By contrast, Figure 9C shows that no detectable *TA56* mRNA was observed within the ablated circular cell cluster region of anthers containing the *TA56/barnase* and *lectin/barstar* genes. A control in situ hybridization experiment with the TP12 anti-mRNA probe produced a strong signal within the connective region at stage 1 similar to that observed with both wild-type

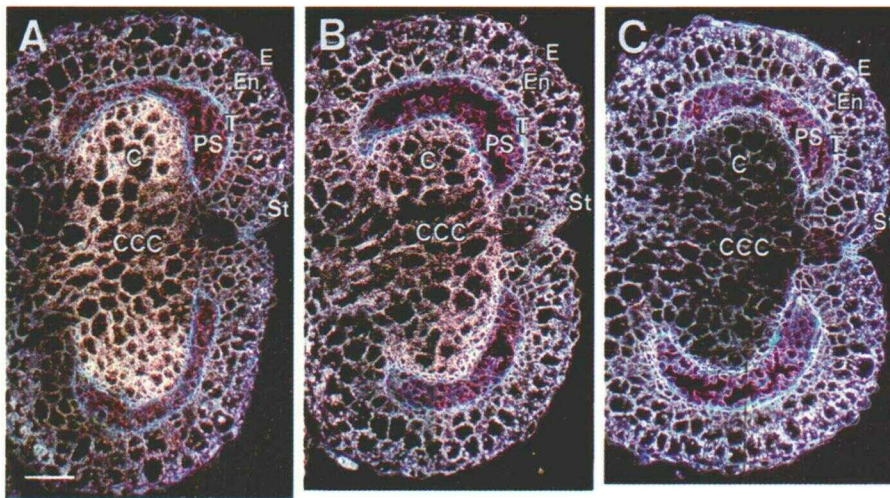


Figure 7. Localization of TP12, Barstar, and Barnase mRNAs in Transgenic Anthers Containing the *TA56/barnase* and *TP12/barstar* Genes.

Stage 4 anthers were fixed, embedded in paraffin, sliced into 10- μ m sections, and hybridized with single-stranded 33 P-RNA probes, as outlined in Methods. Dark-field microscopy was used. Only one theca from each anther is shown.

(A) In situ hybridization with a TP12 anti-mRNA probe. Slide emulsion exposure time was 20 days.

(B) In situ hybridization with a barstar anti-mRNA probe. Slide emulsion exposure time was 90 days.

(C) In situ hybridization with a barnase anti-mRNA probe. Slide emulsion exposure time was 90 days.

C, connective; CCC, circular cell cluster; E, epidermis; En, endothecium; PS, pollen sac; St, stomium; T, tapetum. Bar in (A) = 100 μ m for (A) to (C).

anthers (Figure 7A) and anthers containing the *TA56/barnase* and *TP12/barstar* genes (Figure 7B; data not shown). At stage 2, however, the TP12 hybridization signal was reduced slightly, suggesting that the connective was affected by barnase cytotoxic activity before the effects of ablation could be visualized at the histological level (Figure 2C; data not shown).

We used RT-PCR to show that barnase mRNA was present at stage 4 in anthers containing the *TA56/barnase* and *lectin/barstar* genes (Figure 8, lane 20). By contrast, no detectable barstar mRNA product was observed in the stage 4 anther RNA of these transgenic plants (Figure 8, lane 16), consistent with the weak activity of the 4-kb *lectin* promoter within tobacco anthers (Figure 3C). Similar results were obtained with anther RNA from several independent transgenic lines (data not shown). Control RT-PCR reactions showed that both the TP12 mRNA (Figure 8, lane 4) and the TA56 mRNA (Figure 8, lane 8) were present in stage 4 anthers containing the *TA56/barnase* and *lectin/barstar* genes. The TA56 mRNA product was probably due to endogenous TA56 gene activity within the connective at this developmental stage (Figure 3A; Koltunow et al., 1990). Together, these results indicate (1) that the *lectin/barstar* gene can protect regenerating plants from barnase cytotoxic activity and (2) that the *TA56/barnase* gene can ablate selectively the circular cell cluster, stomium, and adjacent regions at specific stages of anther development.

Anthers Containing the *TA56/barnase* and *lectin/barstar* Genes Fail to Dehisce

We examined the external appearance of anthers containing the *TA56/barnase* and *lectin/barstar* genes to determine whether loss of the circular cell cluster and stomium regions would affect the dehiscence process. Figure 6C shows that a normal-looking stomium notch was visible along the outer edge of the anther at stage 1 similar to that observed in wild-type anthers (Figure 6A) and in anthers containing the *TA56/barnase* and *TP12/barstar* genes (Figure 6B). At stage 3, however, brown patchy areas appeared along the stomium notch, indicating that ablation was occurring (Figure 6C). At later developmental stages, the stomium and contiguous epidermal cells took on a dark brown color (Figure 6C) characteristic of the ablation process observed within the anther cross-sections (Figures 2C and 5C). In striking contrast with wild-type anthers (Figure 6A) and anthers containing the *TA56/barnase* and *TP12/barstar* genes (Figure 6B), anthers containing the *TA56/barnase* and *lectin/barstar* genes did not dehisce at stage 12 when flower opening occurred (Figure 6C). These anthers remained closed even after the flowers had senesced completely and therefore were functionally male sterile (data not shown). Similar results were obtained with all transgenic lines containing the *TA56/barnase* and *lectin/barstar* genes (data not shown).

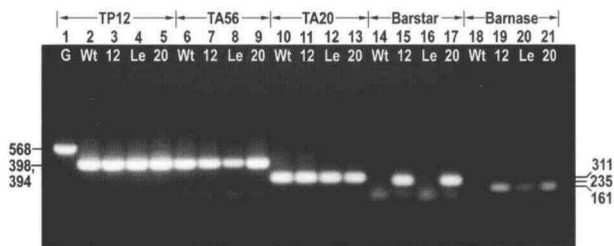


Figure 8. Detection of mRNAs from Wild-Type Anthers and Anthers Containing Chimeric *Barnase* and *Barstar* Genes.

Total RNA was isolated from wild-type anthers and from transgenic anthers containing the *TA56/barnase* and *TP12/barstar* genes, the *TA56/barnase* and *lectin/barstar* genes, and the *TA56/barnase* and *TA20/barstar* genes. Specific mRNA sequences were amplified using RT-PCR, as outlined in Methods. In brief, oligo(dt)₁₅ was annealed with total RNA from anthers at stage 4 and then extended with RT. The cDNA products were amplified with TP12, TA56, TA20, barstar, or barnase PCR primers. Control tobacco genomic DNA was amplified with TP12 PCR primers. Lane 1 shows an amplified 568-bp *TP12* gene fragment from wild-type genomic DNA. This region of the *TP12* gene contains the 398-bp cDNA sequence interrupted by a 170-bp intron (T.P. Beals and R.B. Goldberg, unpublished results). Lanes 2 to 5 contain RT-PCR products from stage 4 anther RNAs from wild-type and transgenic plants amplified with TP12 primers. The predicted PCR product is 398 bp. Lanes 6 to 9 contain RT-PCR products from stage 4 anther RNAs from wild-type and transgenic plants amplified with TA56 primers. The predicted PCR product is 394 bp. Lanes 10 to 13 contain RT-PCR products from stage 4 anther RNAs from wild-type and transgenic plants amplified with TA20 primers. The predicted PCR product is 311 bp. Lanes 14 to 17 contain RT-PCR products from stage 4 anther RNAs from wild-type and transgenic plants amplified with barstar primers. The predicted PCR product is 235 bp. Lanes 18 to 21 contain RT-PCR products from stage 4 anther RNAs from wild-type and transgenic plants amplified with barnase primers. The predicted PCR product is 161 bp. G, genomic DNA; Le, *TA56/barnase* plus *lectin/barstar*; Wt, wild type; 12, *TA56/barnase* plus *TP12/barstar*; 20, *TA56/barnase* plus *TA20/barstar*.

We mechanically opened stage 12 anthers containing the *TA56/barnase* and *lectin/barstar* genes and found no pollen grains (data not shown), which was similar to what was observed at dehiscence with anthers containing the *TA56/barnase* and *TP12/barstar* genes (Figure 6B). Examination of anther cross-sections indicated that tetrads formed and that developing pollen grains degenerated after formation of the exine walls (Figure 2C and data not shown). Capsules were produced when plants containing the *TA56/barnase* and *lectin/barstar* genes were pollinated with wild-type pollen. However, the seeds within these capsules were small, did not contain embryos, and failed to germinate (data not shown), suggesting that these plants were either female sterile or produced embryos that aborted very early in development. Examination of the ovules in one transgenic line by scanning

electron microscopy did not reveal any detectable differences from ovules within the ovaries of wild-type plants (data not shown). In addition, we observed that the *lectin/GUS* gene produces a high level of GUS activity within tobacco ovary tissue (data not shown). We conclude from these results (1) that ablation of the circular cell cluster, stomium, and adjacent connective regions leads to anthers that fail to dehisce and (2) that anthers containing the *TA56/barnase* and *lectin/barstar* genes are both functionally and developmentally male sterile.

The Stomium Is Ablated in Anthers Containing *TA56/barnase* and *TA20/barstar* Genes

We utilized a chimeric *TA20/barstar* gene in combination with the *TA56/barnase* gene to determine whether we could (1) protect a wider range of anther cell types (e.g., connective) from the cytotoxic effects of the *TA56/barnase* gene than that obtained with the *lectin/barstar* gene (Figures 2C and 5C) and (2) selectively ablate either the stomium or the circular cell cluster region. We showed previously that the tobacco *TA20* mRNA accumulates to a high level within many anther cell types, including the connective, during phase two of anther development (Koltunow et al., 1990; T.P. Beals and R.B. Goldberg, unpublished results). In contrast with the *TA56* mRNA, however, *TA20* mRNA does not accumulate to detectable levels within the circular cell cluster (Koltunow et al., 1990; T.P. Beals and R.B. Goldberg, unpublished results). The *TA20* gene has no known counterparts within gene or protein databases available to the general scientific community.

Figure 3D shows that a *TA20/GUS* gene containing a 4-kb *TA20* promoter (see Methods) was active at stage 1 in microspores, tapetum, connective and wall layer cells surrounding the locule, and surprisingly, in the circular cell cluster. At stage 2, and in later stages, *TA20/GUS* activity was very strong in cells surrounding the locule and in most other anther cell types (Figure 3D). Similar patterns of GUS enzyme activity were observed within the anthers of six independent *TA20/GUS* transgenic lines (data not shown).

We fused the 4-kb *TA20* gene promoter to the *barstar* gene, combined the *TA20/barstar* and *TA56/barnase* genes on one plasmid, and introduced the two chimeric genes simultaneously into tobacco cells (see Methods). Many kanamycin-resistant plantlets were regenerated from leaf discs, indicating that similar to the *TP12/barstar* and *lectin/barstar* genes, the *TA20/barstar* gene was a dominant suppressor of *TA56/barnase* gene activity during the transformation and plant regeneration process. We transferred 16 independent lines of kanamycin-resistant plantlets to the greenhouse. DNA gel blot studies showed that each transgenic plant contained from one to three unrearranged copies of the *TA56/barnase* and *TA20/barstar* genes (data not shown). Plants from 15 of the 16 lines containing the *TA56/barnase* and *TA20/barstar* genes resembled both wild-type plants

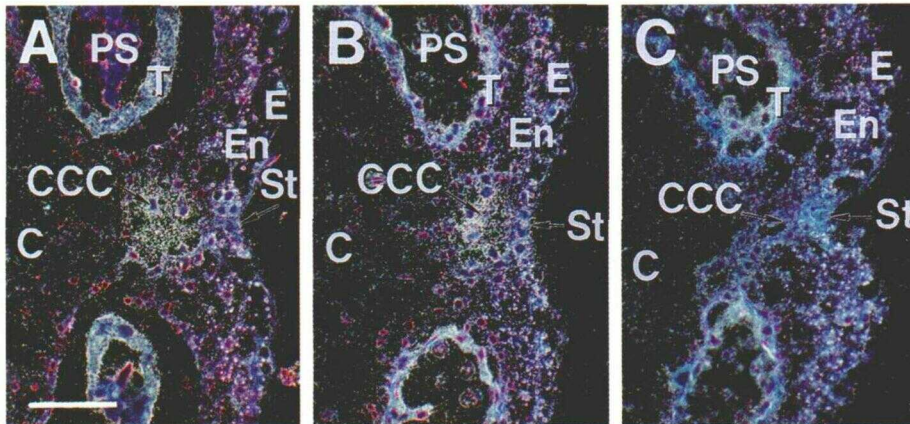


Figure 9. Localization of TA56 mRNA in Wild-Type Anthers and Anthers Containing Chimeric *Barnase* and *Barstar* Genes.

Stage 2 anthers were fixed, embedded in paraffin, sliced into 10- μ m sections, and hybridized with single-stranded 35 S-RNA probes, as outlined in Methods. The sections shown in (A) to (C) were hybridized together on the same slide. Dark-field microscopy was used. Slide emulsion exposure time was 15 days.

(A) In situ hybridization of a TA56 anti-mRNA probe with a wild-type anther.

(B) In situ hybridization of a TA56 anti-mRNA probe with an anther containing the *TA56/barnase* and *TP12/barstar* genes.

(C) In situ hybridization of a TA56 anti-mRNA probe with an anther containing the *TA56/barnase* and *lectin/barstar* genes.

C, connective; CCC, circular cell cluster; E, epidermis; En, endothecium; PS, pollen sac; St, stomium; T, tapetum. Bar in (A) = 50 μ m for (A) to (C).

and plants containing the *TA56/barnase* and *TP12/barstar* genes with respect to height, flowering time, and organ system morphology (data not shown). By contrast, the corolla limb region of one transgenic line failed to develop normally, as was observed within one line containing the *TA56/barnase* and *TP12/barstar* genes (data not shown).

We sectioned anthers containing the *TA56/barnase* and *TA20/barstar* genes to determine whether any anther regions and/or cell types were ablated. Figure 2D shows that anthers containing the *TA56/barnase* and *TA20/barstar* genes developed normally, contained a wild-type set of diverse anther cell types (Figure 2A), and entered a dehiscence pathway, as indicated by the extensive degeneration of the connective at the terminal stages of development (stage 10). High-magnification bright-field photographs shown in Figure 5D indicate that normal-looking circular cell cluster and stomium cells were present in stage 1 anthers and that these cells differentiated as did those in wild-type anthers (Figure 5A) and anthers containing the *TA56/barnase* and *TP12/barstar* genes (Figure 5B). In addition, circular cell cluster degeneration occurred at later stages of anther development within a normal temporal framework (Figures 5A and 5D). Other anther cell types, including those in the tapetum, connective, and endothecium, were also present in anthers containing the *TA56/barnase* and *TA20/barstar* genes (Figures 2D and 5D) and did not differ detectably from similar cells in wild-type anthers at stages 1 to 4 (Figures 2A and 5D). By contrast, the stomium was ablated at stage 10, as indicated by the collapse of cells and loss of nuclei in this region (Figure 5D). Other anther cell types at this developmental stage (Figures 2D and 5D) did not differ detectably from those in

wild-type anthers (Figures 2A and 5A) or anthers containing the *TA56/barnase* and *TP12/barstar* genes (Figures 2B and 5B). Similar results were obtained with anther sections from nine independent transgenic lines containing the *TA56/barnase* and *TA20/barstar* genes (data not shown).

We used RT-PCR to detect directly the presence of barnase and barstar mRNAs in anthers containing the *TA56/barnase* and *TA20/barstar* genes. As shown in Figure 8, RT-PCR products specific for barnase mRNA (Figure 8, lane 21) and barstar mRNA (Figure 8, lane 17) were obtained with stage 4 anther RNA. In addition, RT-PCR products specific for TP12, TA56, and TA20 mRNAs (Figure 8, lanes 5, 9, and 13, respectively) were also obtained with stage 4 anther RNA from plants containing the *TA56/barnase* and *TA20/barstar* genes. Together, these results indicate (1) that the stomium is selectively ablated in anthers containing the *TA56/barnase* and *TA20/barstar* genes and (2) that the *TA20/barstar* gene protects other anther regions, including the circular cell cluster, from the cytotoxic effects of the *TA56/barnase* gene, enabling these regions to develop normally.

Ablation of the Stomium Region Leads to Anthers That Fail to Dehisce

We examined the external appearance of anthers containing the *TA56/barnase* and *TA20/barstar* genes during phase two of anther development. Figure 6D shows that the timing of stomium formation and the structure of the stomium notch separating each theca were similar to those observed with wild-type anthers (Figure 6A) and anthers containing the

TA56/barnase and *TP12/barstar* genes (Figure 6B) throughout most of anther development (stages 1 to 9). In striking contrast with these anthers, however, the stomium notch of anthers containing the *TA56/barnase* and *TA20/barstar* genes had a brownish color characteristic of the ablation process and failed to split at stage 12 when flower opening occurred (Figure 6D).

Anthers of the nine lines containing the *TA56/barnase* and *TA20/barstar* genes studied at the histological level (Figures 2D and 5D) failed to dehisce, as shown in Figure 6D. The anthers of five additional lines did split at the stomium region; however, stomium breakage and dehiscence were never complete (data not shown). Bright-field photographs of anther cross-sections from these five lines showed that the stomium was ablated at stage 10 (data not shown). Anthers from the two remaining *TA56/barnase* and *TA20/barstar* lines transferred to the greenhouse showed extensive necrosis along the edges of the stomium region similar to that observed with anthers containing the *TA56/barnase* and *lectin/barstar* genes (Figure 6C) and failed to dehisce as well (data not shown). Examination of cross-sections of these more severely affected anthers showed that extensive ablation of the stomium, circular cell cluster, and adjacent connective regions occurred and was analogous to that observed in the *TA56/barnase* and *lectin/barstar* anther sections (Figures 2C and 5C).

We opened the *TA56/barnase* and *TA20/barstar* anthers that failed to dehisce and did not find any pollen grains; that is, they were male sterile similar to other anthers containing the *TA56/barnase* gene. Examination of anther sections from plants containing the *TA56/barnase* and *TA20/barstar* genes indicated that tetrads formed and that the developing pollen grains degenerated after formation of the exine wall (Figure 5D and data not shown). Capsules were produced when we pollinated four independent lines containing the *TA56/barnase* and *TA20/barstar* genes with wild-type pollen. Seeds from one line contained embryos that germinated normally, indicating that this line was female fertile. By contrast, seeds obtained from crosses with the other three lines did not germinate. Together, these results indicate that ablation of the stomium late in anther development leads to anthers that fail to dehisce; that is, a functional stomium region is required for normal anther dehiscence.

DISCUSSION

We have used a new strategy for conducting targeted cell ablation studies (Figure 4; Goldberg et al., 1995). This strategy utilizes chimeric *barnase* and *barstar* genes driven by promoters with distinct but overlapping cell specificities (1) to ablate target cells by the production of cell-specific barnase activity and (2) to protect non-target cells by the production of barnase/barstar complexes. Our strategy permits the use of promoters that are active in several different cell

types and/or developmental periods for genetic ablation experiments by using a chimeric *barstar* gene as a dominant suppressor of *barnase* gene cytotoxic activity in non-target cell types. We used the *barnase* and *barstar* genes in combination with promoters that are active in the tobacco anther to investigate regions that play a role in the dehiscence process. Our results show that (1) barnase/barstar complexes can overcome the lethal effects of barnase during the transformation process, permitting the generation of transgenic plants; (2) barnase/barstar complexes can form in most anther cell types; and (3) either selective ablation of the stomium or ablation of the circular cell cluster, stomium, and adjacent connective regions leads to anthers that fail to dehisce.

Chimeric *Barnase* and *Barstar* Genes Driven by Promoters with Overlapping Cell Specificities Can Be Used for Cell Ablation Studies

Targeted cell ablation studies with cytotoxic genes in both plants (Koltunow et al., 1990; Mariani et al., 1990, 1992; Thorsness et al., 1991, 1993; Kandasamy et al., 1993; Goldman et al., 1994; Day and Irish, 1997) and animals (Palmiter et al., 1987; Evans, 1989; O'Kane and Moffat, 1992; Sentry et al., 1993) can provide valuable information with respect to cell function, cell lineage relationships, and interactions between developing cell types. A major limitation of genetic ablation experiments is the requirement for promoters that are active exclusively within the target cell type. Expression of a chimeric cytotoxic gene in non-target cell types can potentially prevent the generation of transgenic organisms or make the results of ablation experiments difficult to interpret. For example, the chimeric cytotoxic gene could act as a dominant lethal during embryo development or have a high toxicity within regenerating plant cells, as we observed when using the *TA56/barnase* gene alone, that is, without a chimeric *barstar* gene partner. In addition, if ablation of the target cell is also correlated with the failure of a neighboring cell to differentiate normally, then this result could be explained by either the loss of an inductive signal from the target cell or the "leaky" expression of the cytotoxic gene in the non-target, neighbor cell type.

Several strategies have been devised to prevent the cytotoxic gene from being active in non-target cell types and/or to ensure that the cytotoxic gene is active within the intended target cell at a specific developmental period (O'Kane and Moffat, 1992; Sentry et al., 1993; Day and Irish, 1997). These include the use of low-activity, attenuated toxins (Bernstein and Breitman, 1989), temperature-sensitive toxins (Bellen et al., 1992; Moffat et al., 1992), or toxins carrying amber mutations that require a tRNA suppressor gene to function (Kunes and Steller, 1991). Conditional cell ablation strategies, however, require cell-specific promoters to be used successfully (Kunes and Steller, 1991; Bellen et al., 1992; Moffat et al., 1992). In addition, use of attenuated

toxins does not prevent ablation of non-target cell types if the promoter is active at elevated levels in the non-target cell (Bernstein and Breitman, 1989). In general, these strategies are limited by the availability of cell-specific promoters and the absence of a "fail-safe" mechanism to protect non-target cell types from ablation.

The *barnase/barstar* dual-gene ablation strategy utilized here overcomes many of these limitations and has several advantages because promoters with multiple cell specificities can be used to drive the cytotoxic gene (Figure 4). First, it is not necessary to use promoters that are active exclusively within the target cell. The target cell only has to be included within the set of cell types in which the promoter is active. Second, the range of cell types that can be investigated by ablation experiments is increased significantly. In principle, any cell type in which a promoter is active can be ablated selectively if other promoters are available with distinct but overlapping cell specificities. Third, chimeric *barstar* genes can be used as general "prophylactics" to protect non-target cells at any developmental stage from the "leaky" effects of *barnase* gene activity. Finally, the results of cell ablation experiments are simpler to interpret because contiguous, non-target cells can be protected from ablation. The only requirements for the *barnase/barstar* dual-gene strategy are that the *barstar* level must be equal to or greater than the *barnase* level in the non-target cell and that there is an excess of *barnase* molecules in the target cell type.

Barnase/Barstar Complexes Can Form in Diverse Plant Cell Types

Barnase is a small ribonuclease (110 amino acids) that functions in the extracellular environment surrounding *B. amyloliquefaciens* cells (Hartley, 1989). Studies in our laboratory and those of others have shown that barnase acts autonomously within (1) the tapetal layer cells of the anther (Mariani et al., 1990), (2) stigmatic cells of the pistil (Goldman et al., 1994), (3) leaf cells (Strittmatter et al., 1995), and (4) ovule cells and maternal tissues of the seed (Colombo et al., 1997). The *TA56/barnase* ablation experiments reported here demonstrate that barnase cytotoxic activity also can occur within regenerating callus and within the connective, endothecium cells, circular cell cluster, and stomium cells of the anther (Figures 2 and 5). In addition, barnase is active within microspore mother cells and/or developing pollen grains because all transgenic lines containing the *TA56/barnase* gene studied here are male sterile (Figure 6), including those that contain the *TP12/barstar* gene, which protects sporophytic cells of the anther from barnase cytotoxic activity (Figures 5B and 6B). Together, these data indicate that barnase functions in a diverse set of plant cell types and is most likely a general phytotoxin.

Barstar is also a small protein (89 amino acids) and forms a one-to-one complex with barnase, inhibiting its ribonuclease activity (Hartley, 1989). Barnase/barstar complexes are very stable, having a K_m of 10^{-14} M (Schreiber and Fersht, 1995).

Barstar is present constitutively within *B. amyloliquefaciens* cells and serves as a general "prophylactic" to protect these bacterial cells from potential cytotoxic activity before secretion of barnase into the extracellular environment (Hartley, 1989).

We showed previously that barnase/barstar complexes form within tapetal cells and protect these cells from barnase cytotoxic activity (Mariani et al., 1992). The experiments reported here demonstrate that barnase/barstar complexes can form in callus cells because the *TP12/barstar*, *lectin/barstar*, and *TA20/barstar* genes act as dominant suppressors of *TA56/barnase* gene activity during the transformation and plant regeneration process. In addition, we infer that barnase/barstar complexes are able to form within most anther cell types because the *TP12/barstar* gene is able to protect the connective, endothecium, circular cell cluster, and stomium from *TA56/barnase* cytotoxic activity (Figures 2B and 5B). Similarly, the *TA20/barstar* gene is able to protect connective, circular cell cluster, and endothecium cells from being ablated by *TA56/barnase* gene activity (Figures 2D and 5D). We conclude from these experiments that barnase/barstar complexes are able to form in the intracellular environments of a diverse number of plant cell types and that the *barnase/barstar* dual-promoter gene strategy outlined here can be used for targeted cell ablation studies with most plant cell types.

Cell-Specific Transcriptional Programs Operate during Anther Development

The anther contains a diverse set of cell types that are functionally distinct and are derived in part from different layers of the stamen primordia (Goldberg et al., 1993, 1995). For example, epidermal cells and their stomium derivatives originate from the L1 layer of the stamen primordia. The wall layers surrounding the locules and, ultimately, pollen grains and sperm cells are derived from the L2 layer. Finally, the connective and vascular bundle (containing xylem and phloem cells) are derived from the L3 layer. How these cell types become differentiated during anther development is not known.

Population hybridization experiments performed in our laboratory with anther nuclear and mRNA populations suggested that most genes expressed specifically within the anther are under transcriptional control (Kamalay and Goldberg, 1980, 1984). Recent experiments by us (Koltunow et al., 1990; Mariani et al., 1990) and by others (Scott et al., 1991) demonstrated that genes specifically expressed within the tapetal cell layer are regulated primarily by transcriptional control processes. For example, both run-off transcription experiments with isolated nuclei and studies with chimeric *GUS* and *RNase* genes showed that the tobacco *TA29* gene is activated specifically within the tapetal cell layer at a specific time in anther development and that tapetal-specific transcriptional control elements can be localized within a 0.25-kb segment of the *TA29* promoter (Koltunow et al., 1990; Mariani et al., 1990).

The experiments reported here show that both the *TA56 thiol endopeptidase* gene and the *TP12 patatin* gene are also regulated by cell-specific transcriptional control events during anther development (Figures 3A and 3B). For example, the spatial and temporal activity of the *TA56* promoter within the anther observed with both the chimeric *TA56/GUS* gene (Figure 3A) and the *TA56/barnase* gene (Figure 5C) is similar to that of the *TA56* mRNA accumulation pattern—that is, transcription occurs first in the circular cell cluster, next in the stomium, and finally in the connective (Koltunow et al., 1990; T.P. Beals and R.B. Goldberg, unpublished results). Similarly, the *TP12* mRNA accumulation pattern within the anther parallels that observed with both the *TP12/GUS* gene (Figure 3B) and the *TP12/barstar* gene (Figure 7B). Collectively, these experiments indicate that there is a diverse set of transcriptional programs that operate during anther development and that each of these programs activates genes in a distinct set of anther cell types. We infer from these results that different anther cell types contain specific transcription factors capable of activating unique anther cell-specific gene sets and that these transcription factors are either localized or activated specifically within the target cell type during anther development. The nature of these cell-specific transcription factors and how they become active in specific cells during anther development remain to be determined.

Previous experiments in our laboratory showed that *TA20* mRNA is not detectable within the circular cell cluster during anther development at the level of sensitivity of *in situ* hybridization experiments (Koltunow et al., 1990; T.P. Beals and R.B. Goldberg, unpublished results). Surprisingly, the experiments reported here for both the *TA20/GUS* gene (Figure 3D) and the *TA20/barstar* gene (Figure 5D) indicate that the 4-kb *TA20* promoter used in our chimeric gene constructions is highly active within the circular cell cluster. We were able to infer that the *TA20/barstar* gene is active within the circular cell cluster because this cell type is protected from *TA56/barnase* cytotoxic activity by the presence of the *TA20/barstar* gene (Figure 5D).

There are several possibilities for the difference between the *TA20* mRNA accumulation pattern and the pattern of *TA20* promoter activity observed here during anther development. First, it is possible that the 4-kb *TA20* promoter region used in our experiments does not contain all of the elements required to program *TA20* transcription within the correct cell types. For example, the 4-kb *TA20* promoter may lack elements necessary to silence *TA20* gene transcription within the circular cell cluster. Second, the *TA20* gene could be regulated primarily at the post-transcriptional level within the circular cell cluster; that is, *TA20* primary transcripts might not be processed and exported to the cytoplasm within cells of the circular cell cluster, or the *TA20* mRNA could turn over rapidly in these cells, or both. Finally, it is possible that the *TA20* promoter is activated early in circular cell cluster development and then silenced at a later period but that both GUS and barstar proteins are relatively

stable and persist within circular cell cluster cells until they degenerate normally during anther development. Regardless of which possibility proves to be the case, cell-specific mRNA accumulation profiles may not always be the best guide for designing ablation experiments using the corresponding gene promoter.

A Functional Stomium Is Required for Anther Dehiscence

One of the most critical aspects of plant reproduction is dehiscence of the anther and release of pollen grains when the flower opens. Mutant anthers that either fail to dehisce or dehisce after the stigma has lost its receptiveness to pollen are male sterile, indicating that specific genes must act during phase two of anther development to enable the anther to split along the stomium and release pollen at the appropriate time (Figure 1; Dawson et al., 1993; Goldberg et al., 1995; P.M. Sanders and R.B. Goldberg, unpublished results). The most striking aspect of the results presented here is that ablation of the stomium leads to anthers that fail to dehisce (Figure 6D). The stomium cells of transgenic lines containing the *TA56/barnase* and *TA20/barstar* genes are ablated selectively during the late stages of anther development (Figure 5D), and loss of the stomium region leads to dehiscenceless anthers; that is, we have been able to use the *barnase/barstar* gene ablation strategy (Figure 4) to generate molecular mutants that phenocopy gene mutations that disrupt the dehiscence process (Dawson et al., 1993). We infer from these results that a functional set of stomium cells is required late in anther development for the dehiscence process to occur and that these cells are programmed genetically to perform stomium-specific functions that are essential for anther dehiscence.

Two important aspects of the dehiscence process remain to be resolved. First, what are the mechanisms responsible for the differentiation of both the stomium cells and the circular cell cluster within the interocular region during anther development, the circular cell cluster and the stomium function independently of each other. Whether they interact with each other and/or with surrounding cell types during phase one of anther development remains to be determined. To answer this question by using the *barnase/barstar* dual-gene ablation strategy (Figure 4) requires stomium- and circular-cell-cluster-specific promoters that are active earlier in anther development than are the promoters described here. Second, how is the release of pollen grains from the anther coordinated with flower development and opening? For example, is there a “coordinating signal” within the flower that is perceived by the stomium and sets off a cascade of dehiscence-specific functions leading to anther splitting along the stomium at the time of flower opening? If so, what is the nature of this signal, and how is it perceived and transmitted to the stomium at the correct time of anther development?

Recent electron microscopy studies of the stomium region during phase two of anther development in our laboratory (P.M. Sanders and R.B. Goldberg, unpublished studies) and in those of others (Bonner and Dickinson, 1989) indicate that the stomium undergoes a cell death and destruction process that is probably responsible for splitting the anther along the stomium region at flower opening. This cell death process does not require the presence of viable pollen grains within the locules because male-sterile anthers generated by tapetal-specific ablation (Koltunow et al., 1990; Mariani et al., 1990) and by the *TA56/barnase* and *TP12/barstar* genes (Figure 6B) dehisce normally. The availability of Arabidopsis anther dehiscence mutants and the *barnase/barstar* dual-gene ablation strategy presented here should enable us to determine the molecular mechanisms responsible for anther dehiscence in the near future.

METHODS

Growth of Plants

Tobacco plants (*Nicotiana tabacum* cv Samsun) were grown in the greenhouse, as described by Kamalay and Goldberg (1980). Stages of tobacco anther development were described elsewhere (Koltunow et al., 1990; Drews et al., 1992). These stages were designated in part using floral bud length as a guide (Koltunow et al., 1990). In our experience, the precise histological events observed within the anther may vary by one or two stages.

Screening of Tobacco Genomic Libraries

A *TA56* genomic clone was isolated from a λ Charon 32 tobacco leaf DNA library by using the *TA56* cDNA clone (GenBank accession number U57825) as a probe (Koltunow et al., 1990). DNA sequencing and gel blot studies indicated that the *TA56* genomic clone contained sequences identical to those in the *TA56* cDNA clone and represented an unrearranged copy of the *TA56* gene that is expressed during anther development (T.P. Beals and R.B. Goldberg, unpublished results). A *TA20* genomic clone was isolated from a λ Dash II (Stratagene) tobacco leaf library by using the *TA20* cDNA clone (GenBank accession number U73165) as a probe (Koltunow et al., 1990). DNA sequencing and gel blot studies indicated that the *TA20* genomic clone contained sequences identical to those in the *TA20* cDNA clone and represented an unrearranged copy of the *TA20* gene that is expressed during anther development (T.P. Beals and R.B. Goldberg, unpublished results).

Construction of Chimeric Genes and Generation of Transgenic Plants

Tobacco plants were transformed with chimeric genes as outlined by Koltunow et al. (1990). The specific details of how each chimeric *barnase* and *barstar* gene plasmid was constructed and a description of these plasmids can be obtained on request.

TA56 Promoter Fusions

A 1.1-kb DNA fragment was isolated from the *TA56* genomic clone and sequenced (GenBank accession number U57824). This DNA fragment contained both *TA56* coding and 5' flanking sequences. The context of the ATG start codon at bases 829 to 831 of the *TA56* DNA sequence was converted into an NcoI site by site-directed mutagenesis, as described previously (Drews et al., 1992). A 0.83-kb *TA56* promoter fragment terminating with the NcoI site at its 3' end was fused with the *Escherichia coli* β -glucuronidase (*GUS*) gene (Jefferson et al., 1987). The same *TA56* promoter fragment was fused with the *Bacillus amyloliquefaciens barnase* gene (Hartley, 1988) that was engineered to contain NcoI and KpnI polylinker sites at its 5' end (Mariani et al., 1990). This resulted in the *TA56* sequence 5'-CC-ATG-GTA-CCG-3' (NcoI, KpnI) followed by nucleotide +30 (G) of the *barnase* gene (Hartley, 1988). The chimeric *TA56/barnase* gene encodes a barnase protein with the translated NcoI and KpnI polylinker sequence Met-Val-Pro at its N terminus fused with barnase at amino acid b3 or -Val (Hartley, 1988). A Ti plasmid *gene 7* 3' end (Dhaese et al., 1983) was added to the *TA56/barnase* gene by using the XbaI site at *barnase* nucleotide +630 (Hartley, 1988; Mariani et al., 1990).

TP12 Promoter Fusions

The chimeric *TP12/GUS* gene was described previously (Drews et al., 1992). The same 2-kb *TP12* promoter fragment present in the *TP12/GUS* gene was fused with the *B. amyloliquefaciens barstar* gene (Hartley, 1988) at an NcoI site introduced at the *barstar* start codon. The NcoI site introduction changed the second amino acid of *barstar* (b2) from Lys to Glu (Hartley, 1988). The Ti plasmid *gene 7* 3' end was added to the *TP12/barstar* gene at the HindIII site of the *barstar* gene at nucleotide +1078 (Hartley, 1988; Mariani et al., 1992). The *TP12/barstar* gene was combined with a plasmid containing the *TA56/barnase* gene, and both chimeric genes were inserted simultaneously into a pGV1500-derived plant transformation vector (Deblaere et al., 1987).

Lectin Promoter Fusions

A 4-kb DNA fragment containing the soybean *Le1 lectin* gene promoter (Goldberg et al., 1983; Vodkin et al., 1983) was fused with the *E. coli GUS* gene (Jefferson et al., 1987). The *GUS* protein encoded by the *lectin/GUS* gene contains the first nine amino acids of lectin at its N terminus followed by six amino acids encoded by the *GUS* gene region immediately upstream of the translation start site. The same 4-kb *lectin* promoter was fused with the *B. amyloliquefaciens barstar* gene containing the Ti plasmid *gene 7* 3' end (Mariani et al., 1992), resulting in a chimeric *lectin/barstar* gene containing the *barstar* gene start codon. The *lectin/barstar* gene was combined with a plasmid containing the *TA56/barnase* gene, and both chimeric genes were transferred simultaneously to the pGV1500-derived plant transformation vector (Deblaere et al., 1987).

TA20 Promoter Fusions

A 4-kb DNA fragment containing the tobacco *TA20* gene promoter was isolated from the *TA20* genomic clone and partially sequenced (GenBank accession number U73164). This DNA fragment contained both *TA20* coding and 5' flanking sequences. The context of the ATG start codon at bases 447 to 449 of the *TA20* DNA sequence was

converted to an NcoI site by site-directed mutagenesis, as described previously (Drews et al., 1992). The 4-kb *TA20* promoter fragment terminating with the NcoI site at its 3' end was fused with the *E. coli GUS* gene (Jefferson et al., 1987). The same *TA20* promoter fragment used in the *TA20/GUS* gene fusion was fused with the same *B. amyloliquefaciens barstar* gene construction used in the *TP12/barstar* fusion. The *TA20/barstar* gene was combined with a plasmid containing the *TA56/barnase* gene, and both chimeric genes were transferred simultaneously to the pGV1500-derived plant transformation vector (Deblaere et al., 1987).

Histochemical Assay for GUS Enzyme Activity

Floral buds were harvested and staged according to previously established morphological criteria (Koltunow et al., 1990; Drews et al., 1992). Anthers were hand-sliced, and sections were stored over wet ice in 100 mM sodium phosphate buffer, pH 7, containing 1 mM EDTA while other anthers were being sectioned. After sectioning was complete, the samples were fixed at room temperature for 30 min in the same buffer containing 1% (w/v) paraformaldehyde. Cut sections sank in the fixative solution, and vacuum infiltration was not applied. Sections were rinsed twice in 50 mM sodium phosphate buffer, pH 7, and then stained for 6 hr at 37°C in 50 mM sodium phosphate buffer, pH 7, containing 0.5% (v/v) Triton X-100 and 2 mM 5-bromo-4-chloro-3-indolyl β -D-glucuronide. After staining, the samples were rinsed and decolorized sequentially in 25, 50, 75, and 100% ethanol. Sections with a thickness of \sim 100 μ m were chosen for photography. These sections were transferred to a well slide filled with 100% ethanol, and a cover slip was placed over the well. The sections were photographed under dark-field illumination by using a \times 10 objective and a \times 3.3 or \times 2.5 camera ocular in an Olympus BH 2 compound microscope (Tokyo, Japan), using an Olympus camera body and AD exposure control unit.

In Situ Hybridization Studies

In situ hybridization was performed as described by Cox and Goldberg (1988) and Yadegari et al. (1994) except that 33 P-RNA probes were used for some experiments. We obtained a lower level of background grains with 33 P-labeled probes in comparison with 35 S-labeled probes, as reported by McLaughlin and Margolskee (1993).

Reverse Transcriptase-Polymerase Chain Reaction

Total RNA was isolated from anthers by using the TRIzol reagent (Gibco BRL), as recommended by the manufacturer. RNA was treated with 2 units of DNase RQ1 (Promega) per μ g for 30 min at 37°C. Twenty picomoles of oligo(dT) (Promega oligo(dT)₁₅) was mixed with 2 μ g of total RNA in a 10- μ L volume of hybridization buffer (0.4 M NaCl, 0.04 M Pipes, 1 mM EDTA; Calzone et al., 1987), heated to 70°C, and then cooled to 25°C over a 2-hr interval. Reverse transcription was conducted in a 20- μ L volume by using SuperScript II modified Moloney murine leukemia virus reverse transcriptase (RT; Gibco BRL), as recommended by the supplier. One-fifth of the RT reaction was amplified by the polymerase chain reaction (PCR) using Taq polymerase, PCR buffer supplied by Perkin Elmer Cetus (Norwalk, CT), and mRNA sequence-specific primers. The following mRNA primers were used: TP12, 5'-CCGCTGCTGCTCCAACCTAT-3' and 5'-GAGGTAATTCGTTTCAGCACCA-3'; TA56, 5'-GAGTTTCGATTTCCACGAAAAG-3' and 5'-AGCAACTCCACATTTGCCTT-3'; TA20, 5'-CTGCCATGAAATTGAATCCT-3' and 5'-TGTGCATGATCCGAAT-

GTCC-3'; barstar, 5'-TCAGAATGATCAGCGACCTCCACC-3' and 5'-AAGTATGATGGTATGTCGCAGCC-3'; and barnase, 5'-CTGGTGGCATCAAAGGGAACC-3' and 5'-TCCGGTCTGAATTTCTGAGCCTG-3' (Strittmatter et al., 1995). PCR-generated fragments were detected by fractionating one-fifth of the PCR reaction volume by electrophoresis in a 1.2% (w/v) agarose gel and staining the gel with ethidium bromide.

ACKNOWLEDGMENTS

We thank our colleagues at Plant Genetic Systems in Gent, Belgium, for advice on the manipulation of the *barnase* and *barstar* genes and for constructing several of the *barnase* and *barstar* plasmids used in our experiments. We are particularly grateful to Prof. Titti Mariani for sharing her knowledge, experience, and insight with the *barnase/barstar* gene system. We thank Dr. Robert Fischer, Dr. John Harada, Dr. Anna Koltunow, and the members of our laboratory for critical reading of the manuscript and for helpful discussions. T.P.B. was supported by a National Institutes of Health Postdoctoral Fellowship. This research was supported by a National Science Foundation grant to R.B.G.

Received June 25, 1997; accepted June 30, 1997.

REFERENCES

- Bellen, H.J., D'Evelyn, D., Harvey, M., and Elledge, S.J. (1992). Isolation of temperature-sensitive diphtheria toxins in yeast and their effects on *Drosophila* cells. *Development* **114**, 787–796.
- Bernstein, A., and Breitman, M. (1989). Genetic ablation in transgenic mice. *Mol. Biol. Med.* **6**, 523–530.
- Bonner, L.J., and Dickinson, H.G. (1989). Anther dehiscence in *Lycopersicon esculentum*. I. Structural aspects. *New Phytol.* **113**, 97–115.
- Bonner, L.J., and Dickinson, H.G. (1990). Anther dehiscence in *Lycopersicon esculentum*. II. Water relations. *New Phytol.* **115**, 367–375.
- Calzone, F.J., Britten, R.J., and Davidson, E.H. (1987). Mapping of gene transcripts by nuclease protection assays and cDNA primer extension. *Methods Enzymol.* **152**, 611–632.
- Colombo, L., Franken, J., Van der Krol, A.R., Wittich, P.E., Dons, H.J.M., and Angenot, G.C. (1997). Downregulation of ovule-specific MADS box genes from petunia results in maternally controlled defects in seed development. *Plant Cell* **9**, 703–715.
- Cox, K.H., and Goldberg, R.B. (1988). Analysis of plant gene expression. In *Plant Molecular Biology: A Practical Approach*, C.H. Shaw, ed (Oxford, UK: IRL Press), pp. 1–34.
- Dawson, J., Wilson, Z.A., Aarts, M.G.M., Braithwaite, A.F., Briarty, L.G., and Mulligan, B.J. (1993). Microspore and pollen development in six male-sterile mutants of *Arabidopsis thaliana*. *Can. J. Bot.* **71**, 629–638.
- Day, C.D., and Irish, V.F. (1997). Cell ablation and the analysis of plant development. *Trends Plant Sci.* **2**, 106–111.
- Deblaere, R., Reynaerts, A., Höfte, H., Hernalsteens, J.-P., Leemans, J., and Van Montagu, M. (1987). Vectors for cloning in plant cells. *Methods Enzymol.* **153**, 277–292.

- Dhaese, P., DeGreve, H., Gielen, J., Seurinck, J., Van Montagu, M., and Schell, J.** (1983). Identification of sequences involved in the polyadenylation of higher plant nuclear transcripts using *Agrobacterium* T-DNA genes as models. *EMBO J.* **2**, 419–426.
- Drews, G.N., Beals, T.P., Bui, A.Q., and Goldberg, R.B.** (1992). Regional and cell-specific gene expression patterns during petal development. *Plant Cell* **4**, 1383–1404.
- Evans, G.A.** (1989). Dissecting mouse development with toxigenetics. *Genes Dev.* **3**, 259–263.
- Goldberg, R.B., Hoschek, G., and Vodkin, L.O.** (1983). An insertion sequence blocks the expression of a soybean lectin gene. *Cell* **33**, 465–475.
- Goldberg, R.B., Beals, T.P., and Sanders, P.M.** (1993). Anther development: Basic principles and practical applications. *Plant Cell* **5**, 1217–1229.
- Goldberg, R.B., Sanders, P.M., and Beals, T.P.** (1995). A novel cell-ablation strategy for studying plant development. *Philos. Trans. R. Soc. Lond. B* **350**, 5–17.
- Goldman, M.H.S., Goldberg, R.B., and Mariani, C.** (1994). Female sterile tobacco plants are produced by stigma-specific cell ablation. *EMBO J.* **13**, 2976–2984.
- Hartley, R.W.** (1988). Barnase and barstar: Expression of its cloned inhibitor permits expression of a cloned ribonuclease. *J. Mol. Biol.* **202**, 913–915.
- Hartley, R.W.** (1989). Barnase and barstar: Two small proteins to fold and fit together. *Trends Biochem. Sci.* **14**, 450–454.
- Horner, H.T., and Wagner, B.L.** (1992). Association of four different calcium crystals in the anther connective tissue and hypodermal stomium of *Capsicum annuum* (Solanaceae) during microsporogenesis. *Am. J. Bot.* **79**, 531–541.
- Jefferson, R.A., Kavanagh, T.A., and Bevan, M.W.** (1987). GUS fusions: β -Glucuronidase as a sensitive and versatile gene fusion marker in higher plants. *EMBO J.* **6**, 3901–3907.
- Kamalay, J.C., and Goldberg, R.B.** (1980). Regulation of structural gene expression in tobacco. *Cell* **19**, 935–946.
- Kamalay, J.C., and Goldberg, R.B.** (1984). Organ-specific nuclear RNAs in tobacco. *Proc. Natl. Acad. Sci. USA* **81**, 2801–2805.
- Kandasamy, M.K., Thorsness, M.K., Rundle, S.J., Goldberg, M.L., Nasrallah, J.B., and Nasrallah, M.E.** (1993). Ablation of papillar cell function in Brassica flowers results in the loss of stigma receptivity to pollination. *Plant Cell* **5**, 263–275.
- Keijzer, C.J.** (1987a). The processes of anther dehiscence and pollen dispersal. I. The opening mechanism of longitudinally dehiscent anthers. *New Phytol.* **105**, 487–498.
- Keijzer, C.J.** (1987b). The processes of anther dehiscence and pollen dispersal. II. The formation and the transfer mechanism of pollenkitt cell-wall development of the loculus tissues and a function of orbicules in pollen dispersal. *New Phytol.* **105**, 499–507.
- Koltunow, A.M., Truettner, J., Cox, K.H., Wallroth, M., and Goldberg, R.B.** (1990). Different temporal and spatial gene expression patterns occur during anther development. *Plant Cell* **2**, 1201–1224.
- Kunes, S., and Steller, H.** (1991). Ablation of *Drosophila* photoreceptor cells by conditional expression of a toxin gene. *Genes Dev.* **5**, 970–983.
- Lindstrom, J.T., Vodkin, L.O., Harding, R.W., and Goeken, R.M.** (1990). Expression of soybean lectin gene deletions in tobacco. *Dev. Genet.* **11**, 160–167.
- Mariani, C., De Beuckeleer, M., Truettner, J., Leemans, J., and Goldberg, R.B.** (1990). Induction of male-sterility in plants by a chimaeric ribonuclease gene. *Nature* **347**, 737–741.
- Mariani, C., Gossele, V., De Beuckeleer, M., De Block, M., Goldberg, R.B., De Greef, W., and Leemans, J.** (1992). A chimaeric ribonuclease-inhibitor gene restores fertility to male sterile plants. *Nature* **357**, 384–387.
- McLaughlin, S.K., and Margolskee, R.F.** (1993). ^{35}S is preferable to ^{35}S for labeling probes used in in situ hybridization. *BioTechniques* **15**, 506–511.
- Moffat, K.G., Gould, J.H., Smith, H.K., and O’Kane, C.J.** (1992). Inducible cell ablation in *Drosophila* by cold-sensitive ricin A chain. *Development* **114**, 681–687.
- Okamoto, J.K., Jofuku, K.D., and Goldberg, R.B.** (1986). Soybean seed lectin gene and flanking nonseed protein genes are developmentally regulated in transformed tobacco plants. *Proc. Natl. Acad. Sci. USA* **83**, 8240–8244.
- O’Kane, C.J., and Moffat, K.G.** (1992). Selective cell ablation and genetic surgery. *Curr. Opin. Genet. Dev.* **2**, 602–607.
- Palmiter, R.D., Behringer, R.R., Quaife, C.J., Maxwell, F., Maxwell, I.H., and Brinster, R.L.** (1987). Cell lineage ablation in transgenic mice by cell-specific expression of a toxin gene. *Cell* **50**, 435–443.
- Schreiber, G., and Fersht, A.R.** (1995). Energetics of protein-protein interactions: Analysis of barnase/barstar interface by single mutations and double mutant cycles. *J. Mol. Biol.* **248**, 478–486.
- Scott, R., Hodge, R., Paul, W., and Draper, J.** (1991). The molecular biology of anther development. *Plant Sci.* **80**, 167–191.
- Sentry, J.W., Yang, M.M., and Kaiser, K.** (1993). Conditional cell ablation in *Drosophila*. *Bioessays* **15**, 491–493.
- Strittmatter, G., Janssens, J., Opsomer, C., and Botterman, J.** (1995). Inhibition of fungal disease development in plants by engineering controlled cell death. *Bio/Technology* **13**, 1085–1089.
- Sulston, J.E., Schierenberg, E., White, J.G., and Thomson, J.N.** (1983). The embryonic cell lineage of the nematode *Caenorhabditis elegans*. *Dev. Biol.* **100**, 64–119.
- Thorsness, M.K., Kandasamy, M.K., Nasrallah, M.E., and Nasrallah, J.B.** (1991). A Brassica S-locus gene promoter targets toxic gene expression and cell-death to the pistil and pollen of transgenic *Nicotiana*. *Dev. Biol.* **143**, 173–184.
- Thorsness, M.K., Kandasamy, M.K., Nasrallah, M.E., and Nasrallah, J.B.** (1993). Genetic ablation of floral cells in Arabidopsis. *Plant Cell* **5**, 253–261.
- Vodkin, L.O., Rhodes, P.R., and Goldberg, R.B.** (1983). A lectin gene insertion has the structural features of a transposable element. *Cell* **34**, 1023–1031.
- Weigel, D., and Meyerowitz, E.M.** (1994). The ABCs of floral homeotic genes. *Cell* **78**, 203–209.
- Yadegari, R.** (1996). Early Embryogenesis in Arabidopsis and Tobacco. PhD Dissertation (Los Angeles, CA: University of California).
- Yadegari, R., de Paiva, G.R., Laux, T., Koltunow, A.M., Apuya, N., Zimmerman, J.L., Fischer, R.L., Harada, J.J., and Goldberg, R.B.** (1994). Cell differentiation and morphogenesis are uncoupled in Arabidopsis *raspberry* embryos. *Plant Cell* **6**, 1713–1729.
- Yanofsky, M.F.** (1995). Floral meristems to floral organs: Genes controlling early events in *Arabidopsis* flower development. *Annu. Rev. Plant Physiol. Plant Mol. Biol.* **46**, 167–188.